Available online at www.sciencedirect.com
SCIENCE DIRECT
Journal of Hydrology 294 (2004) 241–250
Journal of Hydrology
www.elsevier.com/locate/jhydrol

Using remote sensing to regionalize local precipitation recharge rates obtained from the Chloride Method

Philip Brunner*, Peter Bauer, Martin Eugster, Wolfgang Kinzelbach

Institute of Hydromechanics and Water Resources Management, HIL, ETH Hönggerberg Zurich CH-8093, Switzerland

Received 8 May 2003; revised 2 February 2004; accepted 16 February 2004

Abstract

Water supply in semiarid Botswana is, to a large extent, based on groundwater. In the planning of a groundwater abstraction scheme, criteria for the sustainability of the abstraction with respect to both quantity and quality have to be satisfied. The most important parameter in the context of quantitative sustainability is the long-term average groundwater recharge together with its spatial distribution. A method is developed to calculate a recharge map that can be used in a groundwater model. The relative distribution of recharge is obtained from remotely sensed data and then calibrated with local values of recharge derived from the Chloride Method. The method was tested for two sites in Botswana, the Chobe Region and Ngamiland.

Keywords: Groundwater recharge; Chloride method; Remote sensing; Surface water balance

1. Introduction

Several approaches have been developed to quantify groundwater recharge from precipitation. Recharge can directly be measured with lysimeters. This method yields point values over the time the lysimeter is monitored. The costs are high and the time required for installation and monitoring is up to 5 years in semi-arid areas (Lerner et al., 1990). Tracer techniques based on chloride and other environmental tracers such as Tritium or CFC are widely used. Examples of successfully applied tracers can be found in Cook and Herczeg (2000). Tracer techniques usually also yield point values of recharge. Depending on the applied tracer, the recharge estimated is representative for different periods of time. Water balance methods can be used, both at point or catchment scale. A common method consists of calculating recharge rates as the residual from a surface water balance. In humid areas, recharge can be estimated with a satisfactory accuracy by using water balance studies because the magnitude of evapotranspiration is clearly smaller than that of precipitation. In semi-arid or arid areas, groundwater recharge can be smaller than 1% of precipitation, making a reliable recharge estimation from balance methods impossible (Bouwer, 1989). As in these cases, one can in principle obtain the required input data for the surface water balance from satellite imagery data, the spatially resolved recharge patterns can be calculated.

* Corresponding author. Tel.: +41-1633-3082; fax: +41-1633-1061.
E-mail address: brunner@ihw.baug.ethz.ch (P. Brunner).

0022-1694/$ - see front matter
doi:10.1016/j.jhydrol.2004.02.023

Several authors have pointed out the difficulties and importance of the distribution of recharge, e.g. Allison (1988), Edmunds et al. (1994) and Harrington et al. (2002). The spatial and temporal variability is also a very critical parameter for contaminant transport and directly related to the vulnerability of an aquifer system (Robins, 1998). For water management applications the distribution also may be of high interest as emphasized by Scanlon et al. (2002).

For long-term average recharge rates at a specific location, the chloride concentration in the unsaturated soil profile below the zero upward flux plane has been used successfully. If a correlation between recharge rates calculated by the surface water balance and recharge calculated by the chloride mass balance can be found, the recharge map obtained by remote sensing can be used to regionalize the local recharge rates obtained from the chloride concentration in the soil profile or—in a further approximation—in shallow boreholes. Considering the short time span for which remote sensing data are available, a constant recharge pattern in time is the condition under which recharge rates calculated with both methods can be compared.

Two project areas in Botswana were examined to check whether such a correlation exists. The location of the project areas is shown in Fig. 1.

2. Methods

2.1. Surface water balance

The water balance equation for a soil cube of unit cross-sectional area and height d extending from the surface down to the zero upward flux plane is given by:

$$d\frac{\partial \theta}{\partial t} = P - \mathrm{ET} - Q - R \tag{1}$$

where $d =$ height of the soil cube; $\partial\theta/\partial t =$rate of change of the soil water content, $P =$precipitation rate, $ET =$evapotranspiration rate (mm yr^{-1}), $Q =$surface runoff (mm yr^{-1}), and $R =$recharge rate.

For long-term averaged steady-state conditions, the soil water content is constant and consequently its time derivative is zero. For issues of quantitative sustainability only long-term averages are relevant. Hence, steady-state conditions are assumed. With these simplifications the recharge rate can be calculated from precipitation and evapotranspiration. Over permanent water bodies such as rivers or swamps, the assumptions of the simplified water balance do not apply as water is imported or exported by river flow.

As actual ET and precipitation differ only little in semi-arid regions and their absolute value can only be estimated with a large error, no reliable information concerning absolute values of recharge can be obtained by the surface water balance. Still, the resulting

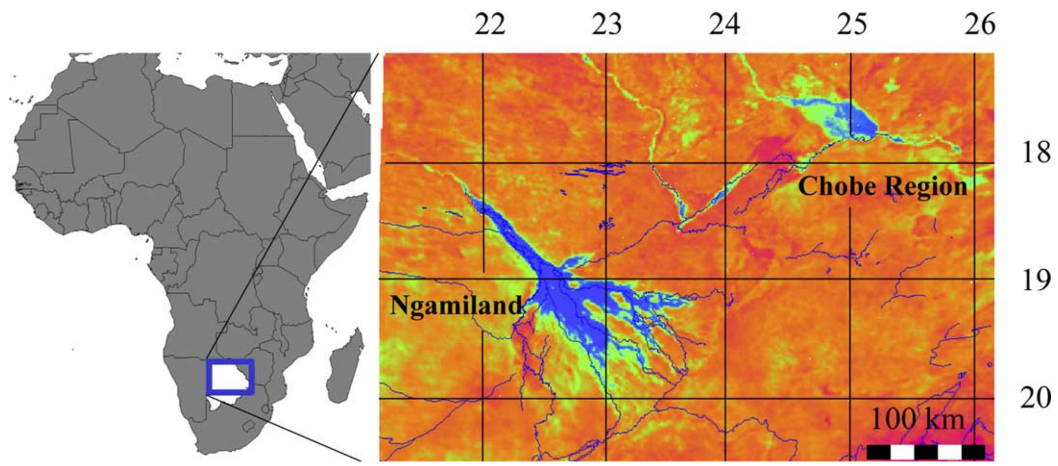

Fig. 1. Location of the study areas (lat-long coordinates).

difference-map (P-ET) can be used for the identification of distinct zones of recharge if such zones show up in a systematic fashion.

2.1.1. Precipitation

The estimation of the accumulated precipitation is based on the GOES Precipitation Index (GPI) algorithm (Herman et al., 1997). Using data provided by the geostationary satellite METEOSAT 5 and rain gauge reports from meteorological stations, precipitation over southern Africa can be estimated with a spatial resolution of 5 km. Rainfall estimates processed by the NOAA Climate Prediction Centre for Famine Early Warning Systems are available for download (www. http://www.cpc.noaa.gov/products/fews/data.html).

2.1.2. Evapotranspiration

Actual evapotranspiration can be written as the product of a reference evapotranspiration and a crop coefficient:

$$\mathrm{ET}_{\mathrm{act}}(x,y,t) = K_{\mathrm{c}}(x,y,t)\mathrm{ET}_{\mathrm{ref}}(t) \tag{2}$$

The crop coefficient was calculated for selected days (Fig. 2) using actual ET as well as reference ET. The resulting values were then interpolated in time. The reference ET is the ET rate for a crop with a defined height as well as defined surface roughness and bulk stomatal resistance. The reference ET can be calculated using the Penman–Monteith equation for the reference crop. In our study, Hargreaves' equation was used instead because it requires only the daily maximum and minimum temperatures as input parameters (Hargreaves and Samani, 1985). Bastiaanssen et al. (1998) calculated actual ET using multispectral satellite images (NOAA-AVHRR) by a surface energy balance algorithm for land (SEBAL). SEBAL requires several input parameters, which were not known with the required accuracy or spatial resolution. Instead of SEBAL, we used a simplified SEBAL algorithm using less parameters described by Roerink et al. (2000). In both approaches, the actual evapotranspiration is written as the product of the average daily net radiation (Rn) and the evaporative fraction (ε). The daily net radiation can be readily calculated from satellite imagery and astronomical data using standard algorithms:

$$\mathrm{ET}_{\mathrm{act}}(x,y,t) = \varepsilon(x,y,t)\overline{\mathrm{Rn}}^{\mathrm{day}}(x,y,t) \tag{3}$$

$$\varepsilon = \frac{\lambda E}{\lambda E + H} = \frac{\lambda E}{\mathrm{Rn} + G_0} \approx \frac{\lambda E}{\mathrm{Rn}}$$

λE is the latent heat flux or the actual ET, H is the sensible heat flux and G_0 is the soil heat flux (all in W m^{-2}). Following Roerink et al. (2000), the evaporative fraction for each pixel of the satellite image can be extracted by plotting all pixels of the image in a coordinate system of surface temperature versus ground albedo (Fig. 3), provided the atmospheric conditions over the project area can be considered constant and the area reflects sufficient variation in surface hydrology conditions.

Roerink's method assumes that pixels close to the line AB are completely wet, their temperature is therefore equal to the blending height temperature and correspondingly, the sensible heat flux is zero.

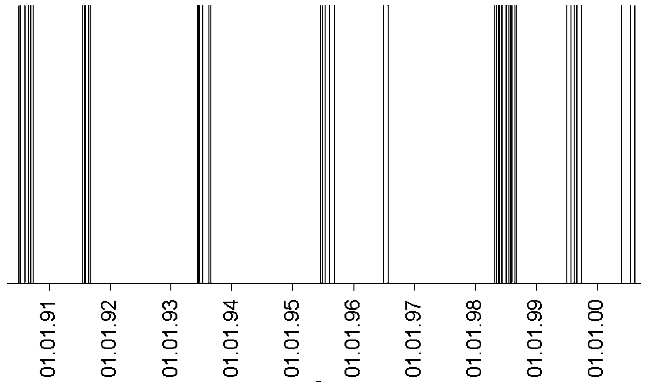

Fig. 2. Temporal availability of processed NOAA-images.

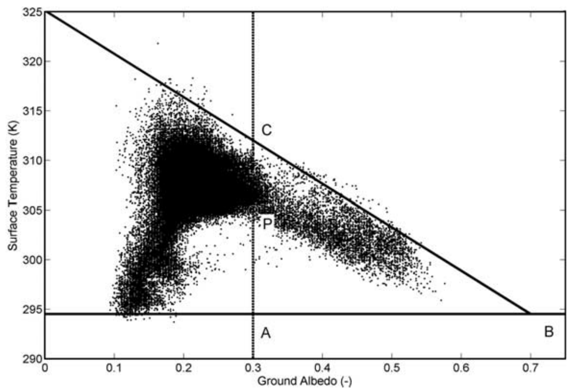

Fig. 3. Example feature space plot for a NOAA-AVHRR image of the project region.

In contrast, pixels close to the line BC are completely dry and the latent heat flux from those pixels is zero. Using a rough model for the atmospheric surface layer by assuming uniform aerodynamic resistance, the evaporative fraction for each pixel can be graphically extracted from the plot. In Fig. 3, the example of a pixel located at P is shown. The evaporative fraction at pixel P is:

$$\varepsilon = \frac{\overline{\mathrm{PC}}}{\overline{\mathrm{AC}}} \tag{4}$$

2.2. Chloride method

Several authors have described the use of chloride in order to estimate recharge (e.g. Allison and Huges, 1978; Edmunds, 1996; Gaye and Edmunds, 1996). The chloride content in groundwater depends on the chloride input by wet and dry deposition, in- or output by lateral groundwater movement, dissolution of chloride from minerals and land use. The chloride deposition from the atmosphere corresponds to the chloride flux into the groundwater under the assumption that the chloride ion is conservative and neither taken up in significant quantities by vegetation, nor dissolved from halites in the subsoil. The Chloride Method is usually applied in the unsaturated soil zone between the groundwater table and the zero upward flux plane. It can, however, in an approximation and under certain limitations (compare Section 4) also be applied between surface and shallow groundwater. Recharge calculated with the chloride mass balance represents a long-term average (Scanlon, 2000).

For steady-state, the recharge rate calculated with the help of the Chloride Method is given by (Gieske, 1992, p. 125):

$$R = \frac{Pc_\mathrm{p} + D}{c_\mathrm{gw}} \tag{5}$$

where R = mean annual recharge rate (m yr^{-1}), P = mean annual rainfall (m yr^{-1}), D = dry deposition rate of chloride (g m^{-2} yr^{-1}), c_p = chloride concentration in the precipitation (g m^{-3}), and c_gw, chloride concentration in the shallow groundwater (g m^{-3}).

3. Site description

The project areas are Ngamiland and the Chobe Region (Fig. 1). Obvious features on the satellite map of Fig. 1 are the Okavango Delta east of Ngamiland and the Chobe-Zambezi River system north of the Chobe Region. The Okavango Delta is a huge wetland system evaporating most of the runoff of the Okavango River. The Chobe-Zambezi River system forms the northern boundary of the Chobe Region.

3.1. Environment

Both sites are located in the Kalahari Desert. The most relevant characteristics of the Kalahari environment for this study are the thick layer of unconsolidated Kalahari sand, geological outcrops and the semi-arid climate. The Kalahari sand forms an up to 300 m thick, uninterrupted sand layer above the lower Kalahari gravels (Davis et al., 1991). In some areas outcrops of fractured rock (Inselbergs) can be found. Examples are the Tsodilo Hills in Ngamiland and the Goha Hills in the Chobe Region. In these regions, the thick sand layer commonly found in the Kalahari is not present. If the sand layer is thin, rainwater infiltrates quickly into the fractured rock where it quickly percolates to larger depths and, therefore, is less exposed to evaporation. Mazor (1982) highlighted that groundwater recharge in the Kalahari is most likely found in zones of high infiltration, e.g. outcrops like the Tsodilo or Goha Hills.

The actual ET reaches the magnitude of potential ET only during the rainy season. In winter, the availability of water is limiting ET. For Kasane, Chobe Region, the potential ET calculated with the Hargreaves equation (Hargreaves and Samani, 1985) yields values ranging from 5 mm d^{-1} in wintertime to 11 mm d^{-1} in summertime (rainy season). Rainfall occurs only during summertime, the mean annual rainfall is approximately 650 mm yr^{-1} (source: meteorological station records, Kasane, Botswana) for Kasane. The clear discrepancy between potential ET and rainfall as well as its distinct temporal distribution is also observed in Ngamiland. Even though single rainfall events may reach high intensities, surface runoff is basically not present. The high infiltration rate of the Kalahari sand, the thickness of the layer and the flat topography inhibit surface runoff in most areas of the Kalahari.

The major local geological and topographical features in the Chobe Region are the Chobe Floodplain, the Chobe forest reserve, the Mababe depression and the Kachikau Fault. The Kachikau fault separates the Chobe Floodplain from the Chobe Forest Reserve. The Floodplain is periodically flooded by the Chobe River. The Chobe Forrest reserve is, like the Chobe Floodplain very flat. The lowest point of the area is the Mababe depression. The Goha Hills are located north of the Mababe Depression. The major geomorphologic features in Ngamiland are the quartzite outcrops of the Tsodilo Hills and the three parallel sand river valleys draining towards the Okavango: the Xudum, Jobo and Quanwa rivers.

3.2. Available data

Climate data: Rainfall as well as minimum and maximum temperatures used for the Hargreaves' equation are regularly recorded at four weather stations in the study area, namely Kasane, Maun, Shakawe and Ghanzi. The most useful source of precipitation data for this study is, as mentioned above, rainfall estimates for time period 1995–2000 based on Meteosat 5 data.

Multispectral images. The NOAA database was searched for cloud free images of the region. In total, 47 NOAA—images between 1990 and 2000 were processed with the method described above. The temporal distribution of the images is shown in Fig. 2.

Chloride. Gieske estimated the total chloride deposition for eight locations in Botswana (Gieske, 1992). The distribution of the chloride deposition is shown in Fig. 4. Over 60 boreholes are located in the Chobe Region, both in the Forest Reserve and in

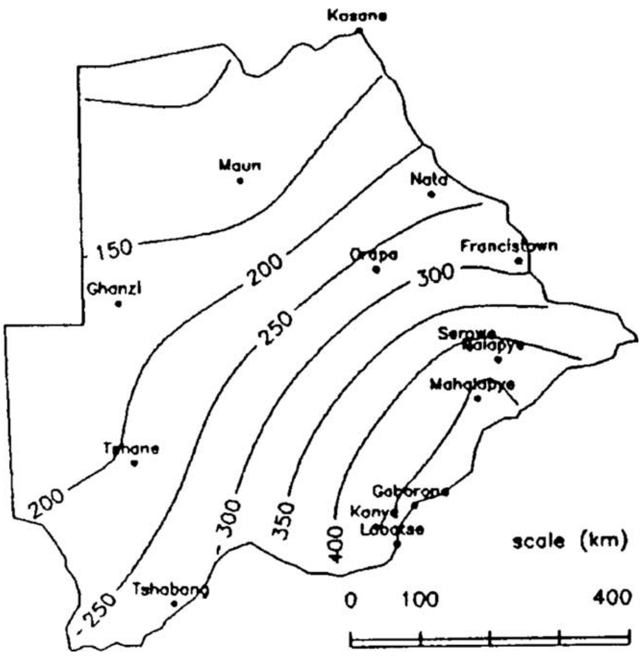

Fig. 4. Distribution of the total chloride deposition over Botswana (mg m^{-2} a^{-1}) after Gieske (1992), p 115.

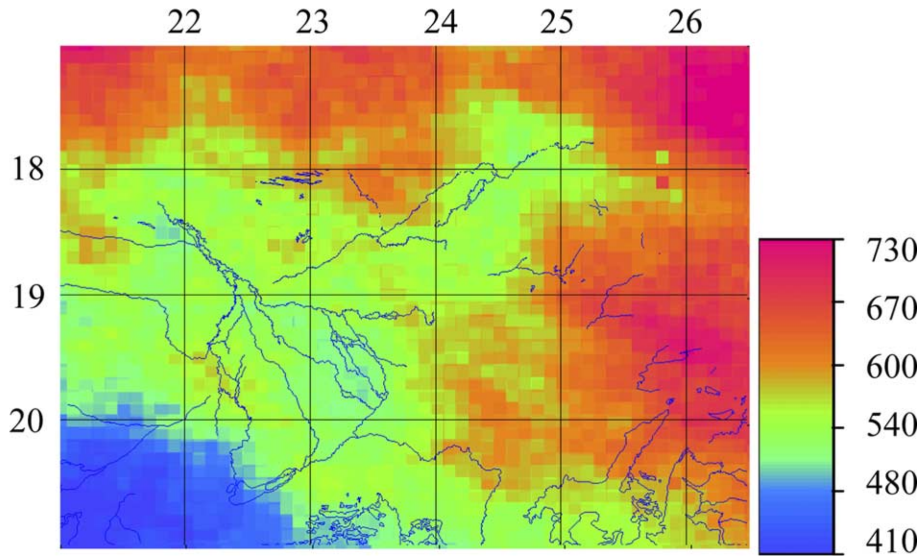

Fig. 5. Average rainfall (1995–2000) over Botswana in mm yr^{-1} based on METEOSAT 5 data as well as rain gauge data. The map covers the same area as the satellite image in Fig. 1. The surface drainage system of Botswana is indicated by the blue lines.

the Chobe Floodplain, and for most of them a chemical analysis is available. In the Chobe Region, no information was available about the depth the samples where taken from. The boreholes are distributed homogeneously over the project area, although more boreholes are found near villages while in the unpopulated areas of the Chobe National Park boreholes are sparse. For Ngamiland, only 10 boreholes were available for this study.

4. Results and discussion

4.1. Surface water balance and Chloride Method

Compared with the measured rainfall in the project region during the same period, the GPI algorithm overestimates rainfall by 17 percent. As we are interested in the distribution of rainfall and not in its absolute value, a further adjustment of rain data estimated with the GPI algorithm is not required. The mean annual precipitation (1995–2000) over the project areas is shown in Fig. 5. A comparison between rain gauge station data in Kasane, Chobe Region and the rainfall estimated over the same area with the GPI algorithm is shown in Fig. 6.

A daily ET rate was calculated for every available NOAA-AVHRR image. Compared to rainfall, evapotranspiration is distributed much more heterogeneously. The time average of the 47 processed ET maps is shown in Fig. 7. Two areas in Fig. 7 should be pointed out. In the Makgadikgadi pans we find very low ET rates. During the rainy season, water accumulates in these pans. As very few NOAA-AVHRR images for the rainy season are available due to cloud cover, ET was systematically underestimated in these areas. A different situation is found

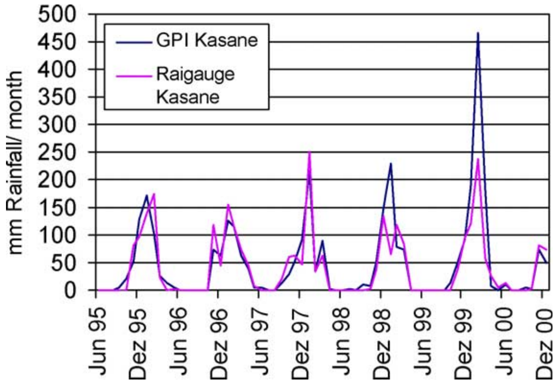

Fig. 6. Rainfall estimates in Kasane with the GPI—algorithm and rain gauge measurements of the local metrological station.

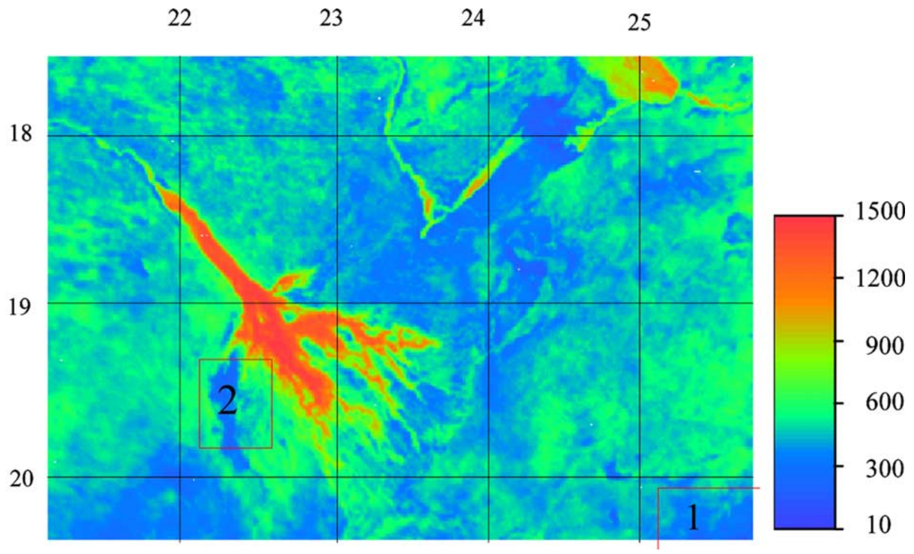

Fig. 7. Resulting map of average evapotranspiration (NOAA images from 1990 to 2000) in mm yr^{-1}. Area 1 shows a part of the Makgadikgadi pans, area 2 is the region of Thaoge river.

in the region of the Thaoge River. The subsurface peat fires in this area cause high surface temperatures, which distort the surface energy balance. As a consequence ET is underestimated. Subsurface peat fires are observed at several locations in and around the Okavango Delta, as described in Ellery et al. (1989). Principal component analysis of over 47 recharge maps (P-ET) showed that the recharge pattern in the project regions remains stable in time. The resulting recharge map (P-ET) is shown in Fig. 8. Due to the unfavourable temporal availability of NOAA-AVHRR images (Fig. 2) ET is systematically underestimated. In the case of the distribution of rainfall no further correction is required as in this study only the spatial distribution of ET is of interest.

Based on the chloride deposition map and the available chloride data from the project areas, recharge rates were calculated with Eq. (5). In principle, recharge rates obtained with the surface water balance and calculated with the chloride mass

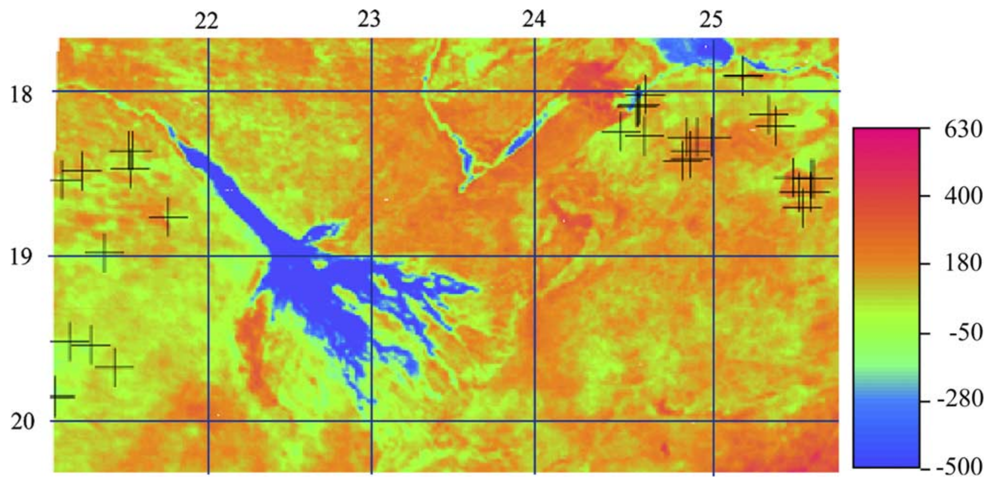

Fig. 8. Resulting map of precipitation minus evapotranspiration (mm yr^{-1}); the crosses represent the boreholes taken into account.

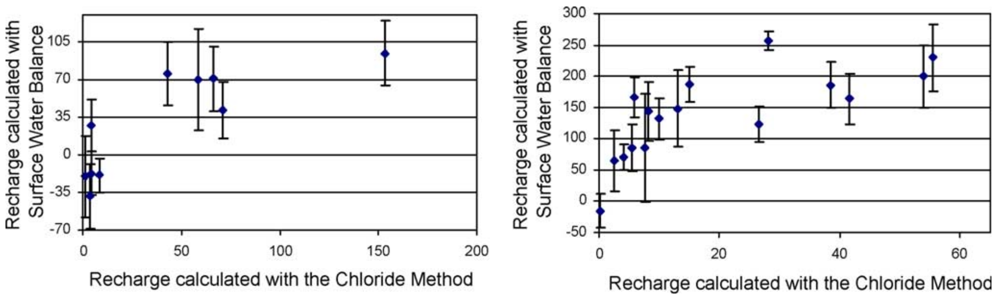

Fig. 9. Plot for Ngamiland (left) and the Chobe Region (right) of recharge calculated with the Chloride Method vs. recharge calculated with the surface water balance. The standard deviations within the averaged pixels used in the water balance method are also plotted.

balance can now be compared. As some boreholes are close together, sometimes even located on the same pixel, it is reasonable to average these boreholes to one single recharge value. This arithmetic averaging reduces the effects of uncertainties of the applied georeference (having an accuracy of 1 km), as well as inaccuracies in the positions of the boreholes. In order to average these boreholes in a consistent way, the pixel size of the surface water balance was increased in several steps and boreholes located on these pixels were arithmetically averaged.

4.2. Comparison of recharge rates

For each resolution, the average recharge rate calculated with the Chloride Method was plotted against the recharge of the pixel (P-ET). Boreholes located on pixels where the assumptions of the surface water balance are not satisfied, e.g. swamps or floodplains like the Chobe Floodplain, are not taken into account. The Chobe Floodplain for example is sporadically flooded and due to the water imports the chloride concentration in the aquifer cannot be used to calculate a long-term recharge rate. The remaining pixels still contain a sufficient number of boreholes to cover nearly the entire range of the recharge quantity (P-ET), as can be seen in Fig. 8.

The average recharge rates calculated with the Chloride Method were plotted against the average of the recharge rates obtained from the water balance of the pixels for several resolutions. For each single plot a linear and a logarithmic regression were performed. In the Chobe Region, a resolution of 8 km × 8 km, in Ngamiland a resolution of 9 km × 9 km showed the clearest trends (Fig. 9). The correlation coefficients are summarized in Table 1.

For the two best resolutions, a Student-*t*-test proved at the 0.05% level that a correlation between the differently calculated recharge rates is statistically significant.

4.3. Scaled recharge map

As a correlation between the recharge estimates has been found, the recharge map obtained from the water balance method can now be scaled according to a regression function. The rescaled recharge map for the Chobe Region is shown in Fig. 10. The results are

Table 1
Summary of correlation coefficients and parameters for both areas

Chobe Region	Linear ($y = ax + b$)	Exponential ($y = a\ln(x) + b$)	Ngamiland	Linear ($y = ax + b$)	Exponential ($y = a\ln(x) + b$)
R^2	0.51	0.74	R^2	0.67	0.78
a	2.6738	39.087	a	0.82	25.314
b	86.395	47.819	b	−5.35	−41.222
Critical *t*-value	2.974		Critical *t*-value	3.25	
t-Value	3.831		*t*-Value	4.001	

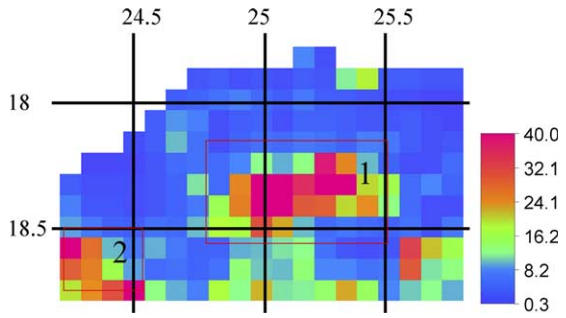

Fig. 10. Rescaled water balance map for the Chobe region (mm yr^{-1}). The pixel resolution is 8 km × 8 km. Rectangle 1 covers the Chobe Forest reserve, rectangle 2 includes the Goha Hills.

in agreement with observed groundwater tables and geological features in the Chobe Region: The highest groundwater tables are found in the areas of high groundwater recharge, namely in the Chobe Forest reserve (Fig. 10) (Brunner et al., 2002). The high recharge values in the southwest are in the area of the Goha Hills. In Ngamiland the highest recharge values from the rescaled map (Fig. 11) are found in the region of the Tsodilo Hills, an outcrop similar to the Goha Hills. The increased recharge rates in the area of these Inselbergs are in agreement with the conclusions of Davis et al. (1991).

The limitations of this approach to calculate recharge lies in the string of assumptions that has to be made. The scaled recharge map should only be

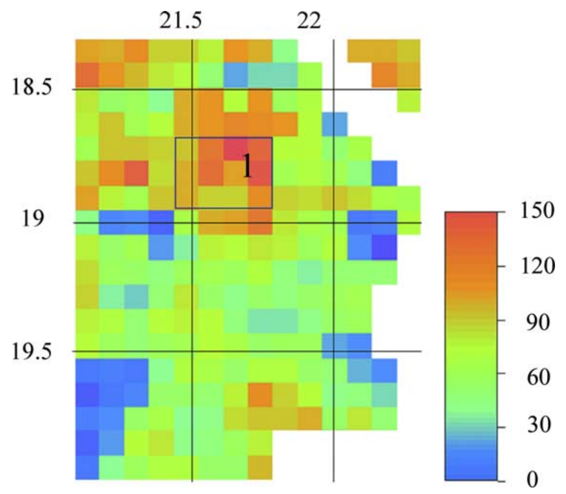

Fig. 11. Rescaled water balance map for Ngamiland (mm yr^{-1}). The pixel resolution is 9 km × 9 km. Area 1 covers the Tsodilo Hills.

calculated for regions where the assumptions for the applicability of both the water balance method and the Chloride Method are fulfilled and a sufficient number of points with chloride measurements are available. It is often difficult to distinguish to which extent these assumptions are fulfilled. In the case of the Chobe Region, a lack of information on the boreholes was causing uncertainties. Additional information about the sampling depth would have allowed screening of the chloride measurements, in order to use only chloride values of the shallow groundwater. This would improve the correlation between the two methods, because the Chloride Method does not apply for deep groundwater. Recharge rates for the shallow groundwater calculated with the chloride mass balance may not represent the recharge rates at sampling location. Instead, they represent an average recharge rate between the point where the water entered the saturated zone and the point the sample was taken (Harrington et al., 2002). If this distance is of a higher magnitude than the spatial extent of a recharge pixel calculated with the surface water balance, the two-recharge rates should not be compared with each other. This problem could distort the final results, especially in areas with high horizontal groundwater gradients or a high variability of recharge rates calculated with the surface water balance. However, the spatial averaging we applied reduces the influence of this type of error.

The assumption of steady state conditions for the water balance equation limits the application of the described method to areas where the water balance did not change significantly for a long time. Like the Chloride Method, this assumption governs the time-scale of the final recharge map, it represents an average recharge rate over a very long time scale. To which extent this assumption is fulfilled may be difficult to determine.

However, if the assumptions of the surface water balance and the Chloride Method are satisfied and precipitation—as well as chloride data are available in the required resolution, the method can easily be adapted to other arid or semi-arid project regions. The multispectral data to calculate ET is available for most countries worldwide. Other tracers than chloride and even lysimeter data in sufficient density could be taken into consideration. The main advantage of this method is that it combines the strong points of two standard approaches. In semi-arid areas recharge rates are the crucial input parameters for groundwater management studies. The calculated standard deviation of the pixel values as well as the extent of correlation between values obtained from the two methods yield important information on the accuracy. This information can be used further for stochastic groundwater modelling. Stochastic models take advantage of the quantified uncertainties of the input data, which propagate into the model results. Examples can be found in Hendricks Franssen et al. (2004) and Kunstmann et al. (2002).

Acknowledgements

We thank the Department of Water Affairs of Botswana without whose support this project would not have been possible. We further gratefully acknowledge financial support received from the Alliance for Global Sustainability.

References

Allison, G.B., 1988. A review of some the physical, chemical, and isotopic techniques available for estimating groundwater recharge. In: Simmers, I., (Ed.), Estimation of natural groundwater recharge, Reidel, Dordrecht.

Allison, G.B., Huges, M.W., 1978. The use of environmental chloride and tritium to estimate total recharge to an unconfined aquifer. Australian Journal Soil Research 16, 181–195.

Bastiaanssen, W.G.M., Menenti, M., Feddes, R.A., et al., 1998. A remote sensing surface energy balance algorithm for land (SEBAL). Journal of Hydrology 212–213, 198–229.

Bouwer, H., 1989. Estimating and enhancing groundwater recharge. In: Sharma, M.L., (Ed.), Groundwater Recharge, Balkema, Rotterdam, Netherlands, p. 1.

Brunner, P., Eugster, M., Bauer, P., Kinzelbach, W., Makobo, P., Carlsson, L., 2002. Assessing the groundwater budget for water supply in an area of low groundwater recharge in northern Botswana, Proceeding of the International Conference on Balancing the Groundwater Budget, 12–17 May, Darwin, Australia.

Cook, P., Herczeg, A.L., 2000. Environmental tracers in subsurface Hydrology, Kluwer Academic Press, Boston.

Davis, S.G., Shaw, T., Shaw, P., 1991. The Kalahari Environment, Cambridge University Press, Cambridge, p. 68 (see also pages 163).

Edmunds, W.M., 1996. Geochemical framework for water quality studies in sub-Saharan Africa. Journal of African Earth Science 22, 385–389.

Edmunds, W.M., Gaye, C.B., 1994. Estimating the spatial variability of groundwater recharge in the Sahel using chloride. Journal of Hydrology 156, 47–59.

Ellery, W.N., Ellery, K., Mccarthy, T.S., et al., 1989. A peat fire in the Okavango Delta, Botswana, and its importance as an ecosystem process. African Journal of Ecology 27, 7–21.

Gaye, C.B., Edmunds, W.M., 1996. Groundwater recharge estimation using chloride, stable isotopes and tritium profiles in the sands of northwestern Senegal. Environmental Geology 27, 246–251.

Gieske, A.S.M., 1992. Dynamics of groundwater recharge. A case study in semi-arid-eastern Botswana. PhD Thesis, Free University of Amsterdam, The Netherlands, 115p.

Hargreaves, G.H., Samani, Z.A., 1985. Reference crop evapotranspiration from temperature. Applied Engineering in Agriculture 1(2), 96–99.

Harrington, G.A., Cook, P.G., Herczeg, A., 2002. Spatial and Temporal Variability of Ground Water Recharge in Central Australia: a Tracer Approach. Ground Water 40(5), 518–528.

Hendricks Franssen, H., Stauffer, H.J., Kinzelbach, F., 2004. Joint estimation of transmissivities and recharges application: stochastic characterization of well capture zones. Accepted for publication in Journal of Hydrology.

Herman, A., Kumar, V.B., Arkin, P.A., 1997. Objectively determined 10-day African rainfall estimates created for famine early warning systems. International Journal of Remote Sensing 18(10), 2147–2159.

Kunstmann, H., Kinzelbach, W., Siegfried, T., 2002. The conditional first order second moment method and its application to the determination of the uncertainty range of groundwater recharge. Water Resources Research 38(4).

Lerner, D.N., Issar, A.S., Simmers, I., 1990. Groundwater recharge—a guide to understanding and estimating natural recharge, International Contributions to Hydrogeology, vol. 8. Verlag, Hannover, 113 pp.

Mazor, E., 1982. Rain recharge in the Kalahari-—a note on some approaches the problem. Journal of Hydrology 55, 137–144.

Robins, N.S., 1998. Recharge: the key to groundwater pollution and aquifer vulnerability. In: Robins, N.S., (Ed.), Special Publications No. 130, Geological Society, London, pp. 1–5.

Roerink, G.J., Su, Z., Mementi, M., 2000. S-SEBI: a simple remote sensing algorithm to estimate the surface energy balance. Physics and Chemistry of the Earth, Part B2 (2), 147–157.

Scanlon, B.R., 2000. Uncertainties in estimating water fluxes and residence times using environmental tracers in an arid unsaturated zone. Water Resources Research 36(2), 395–409.

Scanlon, R.B., Healy, R.W., Cook, P.G., 2002. Choosing appropriate techniques for quantifying groundwater recharge. Hydrology Journal 10, 18–39.